Proceedings of the ASME 2019
Pressure Vessels & Piping Conference
PVP2019
July 14-19, 2019, San Antonio, TX, USA

PVP2019-93502

DESIGN OF AN INTELLIGENT PYTHON CODE FOR VALIDATING CRACK GROWTH EXPONENT BY MONITORING A CRACK OF ZIG-ZAG SHAPE IN A CRACKED PIPE*

Jeffrey T. Fong[1]
National Institute of Standards & Technology
Gaithersburg, MD 20899, U.S.A.

Pedro V. Marcal[2]
MPACT, Corp.
Oak Park, CA 91377, U.S.A.

Robert Rainsberger[3]
XYZ Scientific Applications, Inc.
Pleasant Hill, CA 94523, U.S.A.

N. Alan Heckert[4], **James J. Filliben**[5]
National Institute of Standards & Technology
Gaithersburg, MD 20899, U.S.A.

ABSTRACT

When a small crack is detected in a pressure vessel or piping, we can estimate the fatigue life of the vessel or piping by applying the classical law of fracture mechanics for crack growth if we are certain that the crack growth exponent is correct and the crack geometry is a simple plane. Unfortunately, for an ageing vessel or piping, the degradation will, in practice, change not only the crack growth exponent but the crack shape from a simple plane to a zig-zag pattern. To validate the crack growth exponent for an ageing vessel or piping, we present the design of an Intelligent PYTHON (IP) code to convert the information of the growing crack geometry measured by monitoring a small crack that was initially detected and subsequently continuously monitored over a period of time such that the IP-based analysis code will use the realistic zig-zag crack geometry as a series of re-meshed finite-element meshes for finding the correct crack growth exponent. Using a numerical example, we show that such an IP-assisted continuous monitoring program, using PYTHON as the management tool, TRUEGRID as the topological crack meshing tool, and two finite-element analysis codes for verifiable stress analysis, is feasible for predicting more accurately the fatigue life of a cracked vessel or piping because the material model has a field-validated crack growth exponent. Significance and limitations of this IP-assisted approach are discussed.

Keywords: ageing components; ageing structures; crack growth exponent; crack initiation; crack propagation; NDE; nondestructive evaluation; failure prevention; fatigue modeling; finite element method; fracture mechanics; inspection interval; mathematical modeling; piping; precision structural integrity assessment; pressure vessel; PYTHON; SHM; statistical analysis; stochastic modeling; structural analysis; structural health monitoring; structural integrity; structural reliability; topological crack; TRUEGRID; uncertainty quantification; validation of material property parameters; zig-zag shape of a real crack.

DISCLAIMER

Certain commercial equipment, instruments, materials, or computer software is identified in this paper in order to specify the experimental or computational procedure adequately. Such identification is not intended to imply recommendation or endorsement by the U.S. National Institute of Standards and Technology, nor is it intended to imply that the materials, equipment, or software identified are necessarily the best available for the purpose.

INTRODUCTION

To ensure the safe operation of an engineering structure or system, be it a chemical processing plant, a nuclear power plant, a jet airliner, or a steel bridge, engineers need to first design, manufacture, assemble and install, test in laboratories and in the field, operate with continuous monitoring and scheduled maintenance for all necessary components and connections that are required to make a system work as a whole without failure.

The next task is to estimate the reliability of all such components and connections, construct a fault tree to evaluate the system reliability of the whole structure or system.

Two basic categories of problems of uncertainty come up that require independent study:

(I) Uncertainty in Loads, and

(II) Uncertainty in Resistance.

* Contribution of the U. S. National Institute of Standards and Technology. Not subject to copyright.

In this paper, we restrict ourselves to the study of Category (II), Uncertainty in Resistance, and more specifically, by assuming deterministic loads, we address three types of uncertainty that are essential for predicting the reliability of an ageing component as it operates with a reasonable plan and schedule of inspection and maintenance including the occasional detection and repair of small defects.

The three types of uncertainty are: (1) Material Property *Sampling* Uncertainty (Global). (2) Laboratory-to-Full-Size *Scaling* Uncertainty (Global). (3) Component-specific Life Prediction Uncertainty (Local) based on Continuous Monitoring and Damage-Physics Assessment of a Detected Small Defect.

In Section 1, we briefly describe, using a numerical example, a deterministic formulation of a crack management plan based on classical theory of fracture and fatigue mechanics (see, e.g., Tada, et al. [1], and Dowling [2]), and the emergence of a practical approach to monitor cracks, either continuously or intermittently, to prevent premature failures (see, e.g., Chang [3], Giurgiutiu [4], and Fong, Ranson III, Vachon, and Marcal [5]).

In Section 2, we present two uncertainty studies to show that the deterministic crack management plan is flawed because it fails to account for the uncertainty in two measurable quantities, namely, (a) the crack growth exponent (see Fong, et al. [6], von Euw, et al. [7], and Kanninen and Popelar [8]), and (b) the lower limit of the length of a crack that is detectable and measurable (see Fong, Heckert, Filliben, and Doctor [9]). Since the problem of predicting the life of a specific component requires an assessment of the local damage physics, whereas the two uncertainty studies were "global" in nature, a better approach to bridge the gap from global physics to local must be found to assure the safe operation of individual components and the system as a whole.

In Section 3, we present two arguments to show why the problem is best solved by using a combination of sensor technology and advanced analysis and local physics adaptive modeling technique, otherwise known as the "Intelligent PYTHON (IP) code." This is followed in Section 4 by the development of a new finite element meshing technique known as a "topological crack," which is capable of mimicking a real crack of a zig-zag or irregular shape. In Sections 5 and 6, we show with a numerical example that it is feasible to link an IP code with a structural health monitoring (SHM) code to yield an early warning signal for an ageing component in service with a known small defect. A discussion of our results and some concluding remarks are given in Sections 7 and 8, respectively.

1. A Deterministic Crack Management Plan

As shown in Fig. 1, the classical theory of fatigue based on a crack-length and stress-intensity-versus-yielding approach yields a deterministic crack management plan, where the remaining service (fatigue) life of a component, N_{if} , from an initial state (i) when a crack was first detected with length, a_d ($= a_i$), to a hypothetical final state (f) defined by the existence of a critical crack length, a_c ($= a_f$) when catastrophic failure occurs, is given by the following formula ($\Delta S = S_{max} - S_{min}$):

$$N_{if} = \frac{a_f^{1-m/2} - a_i^{1-m/2}}{C\left(F\ \Delta S\sqrt{\pi}\right)^m (1-m/2)} \qquad (m \neq 2) \quad , \tag{1}$$

where m is the crack growth exponent from the da/dN vs. ΔK plot, C , the modified y-intercept (C_1) of the plot with an empirical material-dependent correction for the mean stress effect, and F, a purely crack-geometry-dependent dimensionless

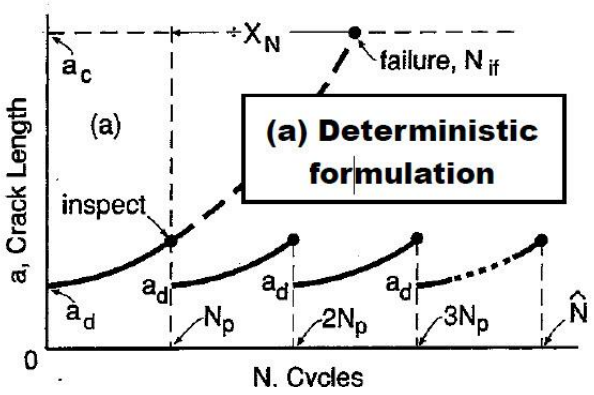

FIGURE 1: An application of the so-called crack-length-based approach to fatigue modeling and crack management (after Dowling [2, p. 491, Fig. 11.2]) provides the basis for the above plot (a) Deterministic Formulation of a Scheduled Inspection Interval Plan, where the length of a growing crack, a , found in a component, is plotted against the number of cycles, N , for that component with an initially detected crack length, a_d , a critical crack length, a_c , and an interval of inspection measured by the number of cycles, N_p , such that the crack length at the end of each scheduled inspection is reduced by the maintenance crew to the lowest detectable crack length. The interval, N_p , is estimated using Eq. (1) and a design safety factor.

positive "fudge" factor, greater than 1.0, that depends on the ratio of the crack length to another geometric dimension (e.g., for a crack in an infinite plate, $F = 1.0$, as shown in Dowling [2, p. 301, Fig. 8.12]).

Note that Eq. (1) assumes constant amplitude loading with fixed maximum and minimum cyclic stresses, S_{max} and S_{min} . Under the condition that the four parameters, ΔS (loading), F (geometry), m and C (material properties), are all constant, it is possible to use Eq. (1) to evaluate an incremental life, N_{12} , from stage-*1* to stage-*2* if a structural health monitoring (SHM) system reports a crack length, a_1 (replacing a_i) at stage-*1*, and another crack length, a_2 (replacing a_f) after N_{12} cycles of loading are completed at stage-*2*.

Better still, if the SHM system is able to report, either continuously or intermittently, a sequence of crack length vs. cycles data (a vs. N), one can easily calculate da/dN and its inverse, dN/da , as a function of N , such that a plot of dN/da

vs. N , as shown in Fig. 2, yields the result that the area under the curve equals the fatigue life, N_{if} . Such a plot is very interesting in the sense that one can obtain an estimate of N_{if} from the output of an SHM system and an assumption of a_f without knowing the one geometric, one loading, and two material property parameters of Eq. (1).

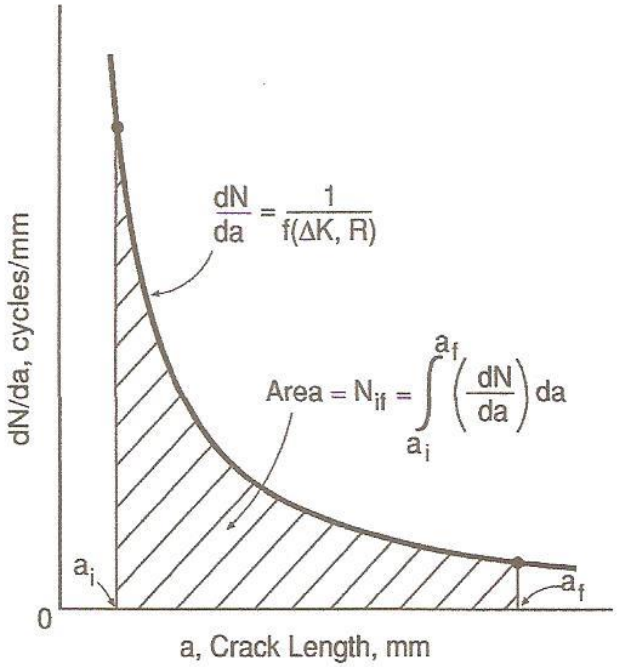

FIGURE 2: Area under the dN/da (which is the inverse of da/dN) vs. a curve used to estimate the number of cycles to grow a crack from initial size a_i to final size a_f (after Dowling [2, p. 521, Fig. 11.26]).

To understand the subtleties of applying Eq. (1), and to pave the way for us to perform an uncertainty analysis of the relationship between the fatigue life, N_{if} , and the crack growth exponent, m , we reproduce below a summary of a textbook exercise given by Dowling [2, pp. 522-524, Example 11.4]:

Given: (100 - 106 Material Properties)

(100) AISI 4340 Steel at room temperature.
(101) σ_o (yield) = 1255 MPa.
(102) σ_u (ultimate strength) = 1296 MPa.
(103) K_{IC} = 130 MPa$\sqrt{m}$.
(104) m (crack-growth exponent) = 3.24.
(105) C_1 = 5.11 x 10^{-10} (unit omitted for brevity).
(106) γ = 0.420.

(200 - 204 Cracked Component Geometry)
(200) A center-cracked plate (see Ref. [2, Fig. 8.12(a)].
(201) b = 38 mm.
(202) t = 6 mm.
(203) a_i = 1 mm. (204) a_f = To be determined.

(300 - 302 Loading)
(300) Tension-to-tension cyclic loading.
(301) P_{min} (minimum applied load) = 80 kN.
(302) P_{max} (maximum applied load) = 240 kN.

To find: (a) At what crack length a_f is failure expected? Is the cause of failure yielding or brittle fracture?
(b) How many cycles can be applied before failure occurs?

Answer: (a) The crack length at fully plastic yielding is estimated to be 22.1 mm (calculation omitted for brevity). The crack length at brittle fracture is estimated as 15.8 mm (calculation also omitted for brevity). The cause of failure is, therefore, brittle fracture.

(b) To apply Eq. (1) with a_i = 1.0 mm, a_f = 15.8 mm, we need to estimate the following:

(401) F = 1.03 (calculation omitted for brevity).
(402) R = P_{min} / P_{max} = 80 / 240 = 0.333.
(403) C = C (C_1, m, γ) = 1.095 x 10^{-12} (unit omitted for brevity).
(404) S_{max} = P_{max} / $2bt$ = 526 MPa.
(405) ΔS = S_{max} ($1 - R$) = 351 MPa.
(406) (1 - m/2) = - 0.62.

Substituting all the various numerical values of parameters in Eq. (1) finally gives N_{if} as follows:

Answer (b): N_{if} = 70,600 cycles. (2)

2. A Simplified Uncertainty Analysis of Equation (1)

An examination of both Eq. (1) and the details of an application example given in the last section shows that the fatigue life, N_{if} , depends on at least 12 parameters, of which 6 are of material property, 4 , geometric, and 2 , of a loading nature. A full uncertainty analysis of Eq. (1), based on the classical law of propagation of errors in the statistics literature (see, e.g., Ku [10]) is feasible and will be given in the later part of this section. What is interesting for a start is to examine the change of N_{if} due to a small change, say, 5 % , in the crack-growth exponent m , using the numerical example of an application of Eq. (1) in the last section with all other parameters being held constant.

Given: (100 - 106 Material Properties)

(100) AISI 4340 Steel at room temperature.
(101) σ_o (yield) = 1255 MPa.
(102) σ_u (ultimate strength) = 1296 MPa.

(103) K_{IC} = 130 MPa√m.
(104) m = 3.24 x 1.05 = 3.40 (This is new.)
(105) C_1 = 5.11 x 10^{-10} (unit omitted for brevity).
(106) γ = 0.420.

(200 - 204 Cracked Component Geometry)
(200) A center-cracked plate (see Ref. [2, Fig. 8.12(a)].
(201) b = 38 mm.
(202) t = 6 mm.
(203) a_i = 1.0 mm.
(204) a_f = 15.8 mm (from answer (a) in Section 1).

(300 - 302 Loading)
(300) Tension-to-tension cyclic loading.
(301) P_{min} (minimum applied load) = 80 kN.
(302) P_{max} (maximum applied load) = 240 kN.

To find: (b) How many cycles can be applied before failure occurs?

Answer (b): **N_{if} = 40,200 cycles**. (3)

A comparison of the results in Eqs. (2) and (3) shows that a + 5 % change in the crack-growth exponent, m, can lead to a decrease in life, N_{if}, of 30,400 cycles, or, - 43 %. This is alarmingly high, and not acceptable, since it is well-known in the literature that the crack-growth exponents for most metal alloys have a broad scatter band (see Fig. 3).

Another parameter of interest to an uncertainty analysis of Eq. (1) is the initial crack length, a_i. A visual inspection of Fig. 2 yields the conclusion that a change of a_i, say, from 1 mm to 2 mm can lead to a major change in the area under the curve, i.e., the fatigue life, N_{if}, because the ordinate of a is clearly the largest at $a = a_i$. As shown in Fig. 4, a stochastic crack management plan can easily be developed to assist an SHM system as recently demonstrated by Fong, et al. [6].

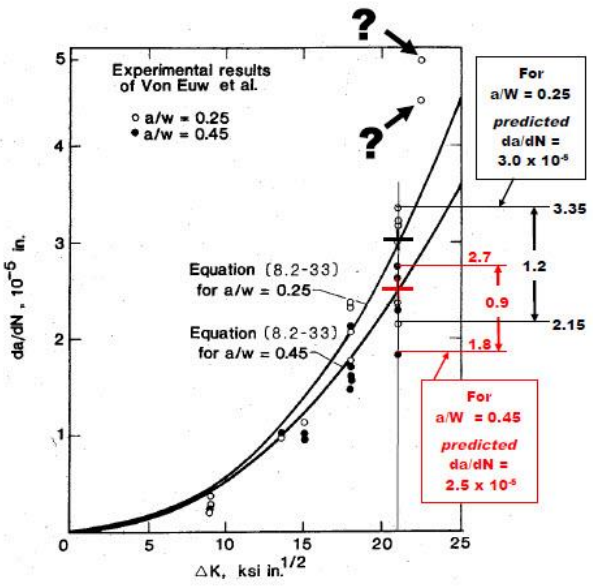

FIGURE 3: Comparison of predicted and experimental fatigue crack growth results in 2024-T3 aluminum alloy for R = 0 (after von Euw, Hertzberg, and Roberts [7] as captioned by Kanninen and Popelar [8, p. 522], and further analyzed by Fong, Marcal, Hedden, Chao, and Lam [6]). Note the broad spread of the experimental da/dN dta between 2.15x10^{-5} and 3.35x10^{-5} for ΔK = 21, and a/W = 0.25. Similar scatter also appears (in red) for a/W = 0.45.

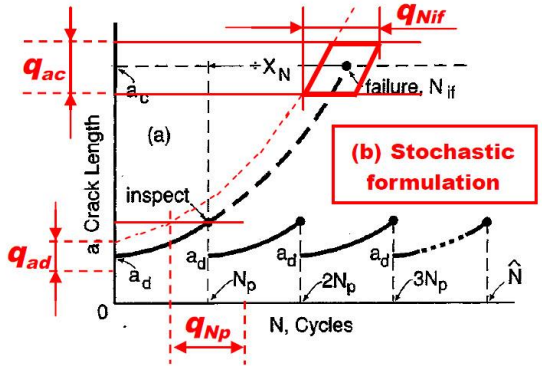

FIGURE 4: A new application of the so-called crack-length-based approach to fatigue modeling and crack management (after Dowling [2], and Fong, et al. [6]) provides the basis for the above plot (b) Stochastic Formulation of a Scheduled Inspection Interval Plan, where the length of a growing crack, a, found in a component, is plotted against the number of cycles, N, for that component with an initially detected crack length, a_d, with uncertainty, +/- q_{ad} /2, a critical crack length, a_c, with uncertainty, +/- q_{ac} /2, and an interval of inspection measured by the number of cycles, N_p, with uncertainty, +/- q_{Np} /2, such that the crack length at the end of each scheduled inspection is reduced by the maintenance crew to the lowest detectable crack length.

Before we conduct a full uncertainty analysis of Eq. (1) using the theory of error propagation [10], let us re-examine the form of the equation, where the fatigue life, N_{if}, supposedly depends on 6 material property, 4 geometric, and 2 loading parameters as listed in Sect. 1.

First of all, we observe that some of the parameters are not totally independent, as for example in the case of the final crack length, a_f, which depends on three of the six material property parameters, namely, the yield strength, the ultimate strength, and the critical stress intensity factor.

Secondly, we can simplify the equation by discarding the term involving the final crack length, a_f, because, according to the observation made in Fig. 2 of the last section, the contribution of the term involving a_f is negligibly small as compared with that involving the initial crack length, a_i. Consequently, for the study of the uncertainty of the fatigue life, it is reasonable to use a simplified form of Eq. (1) by discarding the term involving a_f, the final crack length, as shown below:

$$N_{if} \approx a_i^{(1-m/2)} / \{ C (F \Delta S \sqrt{\pi})^m (m/2 - 1) \}, \quad (2)$$

where we are left with only five parameters, a_i, m, C, F, and ΔS, of which three. i.e,, C, F, and ΔS, may be assumed constant for the simplified uncertainty analysis. In other words, Eq. (2) may be re-written as a function of two variables, a_i, and m, as follows:

$$N_{if}(a_i, m) = a_i^{(1-m/2)} / \{ C (H)^m (m/2 - 1) \}, \quad (3)$$

where $H = F \Delta S \sqrt{\pi}$. Taking the natural logarithm of both sides of Eq. (3), we obtain,

$$Ln(Nif) = (1 - m/2) Ln(a_i) - Ln(C) - m Ln(H) - Ln(m/2 - 1). \quad (4)$$

Let us re-order the five terms on the right hand side of Eq. (4) as follows:

$$Ln(Nif) = - Ln(C) - m Ln(H) - Ln(m/2 - 1) + Ln(a_i) - (m/2) Ln(a_i), \quad (5)$$

Where the first term is a constant, the second, a linear term involving the variable m, the third and fourth terms, two log terms each involving one of two variables, m and a_i, and the fifth term, a product of the variable m with the log of the other variable, a_i.

We are now ready to apply the error propagation formulas listed in Ku [10] to obtain a relationship between the variance of N_{if} and the variances of m and a_i. More specifically, we need the formulas for the variances of the sum and the product of two variables, and the natural logarithm of a single variable. Let X and Y be two random variables, Xbar and sdX denote the mean and standard deviation of X, respectively, and var(X), the variance of X that is equal to the square of sdX. The following three formulas are reproduced from Ku [10]:

$$\text{(Sum)} \quad \text{var}(AX+BY) = A^2\text{var}(X) + B^2\text{var}(Y). \quad (6)$$

$$\text{(Prod.)} \quad \text{var}(X Y) = \text{Ybar}^2\text{var}(X) + \text{Xbar}^2\text{var}(Y). \quad (7)$$

$$\text{(Log}_e\text{X or Ln(X))} \quad \text{var}(\text{Ln}(X)) = \text{var}(X)/ \text{Xbar}^2. \quad (8)$$

Repeated applications of the above three formulas to the uncertainty quantification of Eq. (5) yields the following result:

$$\{\text{cv}(N_{if})\}^2 = (1 + m^2/4) \{\text{cv}(a_i)\}^2 + \{[(m/2)Ln(ai)]^2 + [mLn(H)]^2 + [m/(2-m)]^2\} \{\text{cv}(m)\}^2, \quad (9)$$

where cv(X) is the coefficient of variation of the variable X, defined by the following relation,

$$\text{cv}(X) = \text{sdX}/\text{Xbar}, \text{ or, } \text{cv}(X)^2 = \text{var}(X)/\text{Xbar}^2. \quad (10)$$

It is interesting to observe that Eq. (9) resembles a weighted Pythagoras formula with the term, $\text{cv}(N_{if})$, acting as the hypotenuse of a right-angled triangle.

We are now ready to verify a numerical result that was computed in the early part of this section that a small change of the crack growth exponent, m, yields a shockingly large change in the remaining fatigue life, Nif. For the example cited earlier on an AISI 4030 steel specimen at room temperature in a cyclic loading, Eq. (9) becomes,

$$\{\text{cv}(N_{if})\}^2 = 3.6 \{\text{cv}(a_i)\}^2 + 566 \{\text{cv}(m)\}^2, \quad (11)$$

or,

$$\text{cv}(N_{if}) \approx 23.8 \text{ cv(m)}, \quad (12)$$

if we neglect the uncertainty in the measurement of the initial crack length and focus only on that of the crack growth exponent.

3. Why Design An Intelligent PYTHON (IP) Code?

Having developed a stochastic crack management plan as shown in Fig. 4, we show in this section why and how to design an intelligent PYTHON (IP) code to turn an SHM system into a "precision" structural integrity assessment tool.

About a decade ago, an IP code to assist non-destructive examination (NDE) personnel in their field-detection and measurement of weld flaws was developed by Fong, Hedden, Filliben, and Heckert [11], another to assist designers of fire-resistant structures to access huge databases of material properties at high temperatures was developed by Fong and Marcal [12], and a third to assist reliability engineers to access failure data scattered around the world was done by Fong, Marcal, and Yamagata [13].

Today, as demonstrated by Neapolitan and Jiang [14], Boobier [15], Chollet [16], etc., IP is a special type of artificial intelligence (AI), which can help engineers turn old imprecise methods (based primarily on small-sample and globally-acquired information) to new "precision" tools that can be tailored to the assessment of the health of individual components (requiring highly specific "local" information). An example of this trend was recently given by Frolov [17], where he applied AI and machine learning to empower models for digital twins based on advanced sensor technology.

Consequently, in light of the above, let us first answer the question,

> *"Why do we need IP to alleviate the uncertainty problem in fatigue life prediction?"*

and then proceed to show how an IP code could be developed to solve the uncertainty problem.

To answer the "why" question, we need to first identify a major knowledge gap between (A) what we knew about a component when it first went into service, and (B) what we now know about that component after years of service. Knowledge (A) consisted of information we collected from handbooks and by sampling and scaling (global data) with statistical bounds of uncertainty that were seldom documented, while Knowledge (B) on an ageing component is practically non-existent, because no one is willing to cut several pieces of that component for testing to see how much damage has resulted from years of service.

Fortunately, advanced sensor technology and the development of SHM systems made Knowledge (B) richer, so our *first argument* is that

> "*we need to discover "local damage physics' from SHM-generated data by intelligently 'guessing' and subsequently 'validating' key parameters in Eq. (1)."*

Unfortunately that first argument is not good enough, because when we look at all the tools and methods in fracture mechanics [1, 2, 7, 8], very few are applicable to real cracks, i.e., most tools deal with idealized cracks that are plane in geometry. For example, real cracks that are formed by void growth have irregular shapes that are zig-zag in nature (see, e.g., Fig. 5 after Osovski, Srivastava, Ponson, Bouchaud, Tvergaard, Ravi-Chandar and Needleman [18]).

So our *second argument* for using IP tools to discover "local damage physics" is that

> *"We need to adopt PYTHON as a management tool to activate a large number of simulation codes of different platforms such that we could intelligently 're-mesh' the entire component, particularly in the vicinity of the crack tip which is moving in time, and perform a nonlinear finite element stress analysis with the newly-discovered 'local damage physics' to yield solutions that can be verified every step of the way when a crack is advancing."*

With those two arguments, we are convinced that only through IP are we able to turn an SHM system into a "precision" structural integrity assessment tool.

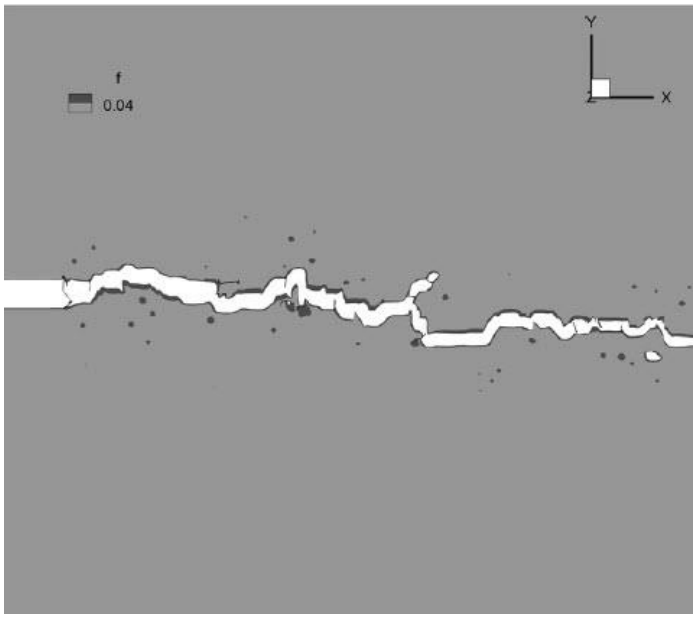

FIGURE 5: A typical computer-simulated crack due to void-by-void growth at a relatively low loading rate of 1×10^5 MPa$\sqrt{m}$ s^{-1} (after Osovski, Srivastava, Ponson, Bouchaud, Tvergaard, Ravi-Chandar and Needleman [18]), shows the zig-zag shape of cracks found in many real components.

4. Finite Element Meshing of a Real Crack

To discover "local damage physics" in a specific ageing component and to predict with greater confidence its remaining fatigue life, N_{if} , using early-reported SHM data, we rely on closed-form formulas such as Eq. (1) and numerical simulation tools such as the finite element method (FEM).

A pre-requisite in using FEM is the ability to design finite element meshes of high quality and near "optimal" density distribution to assure the achievement of accurate results at a reasonable cost and time. For example, using an FEM preprocessor named TRUEGRID, Rainsberger, Fong, and Marcal [19, 20] recently showed that high-quality and optimally-balanced mesh designs with quadratic 10-node tetrahedron or 27-node hexahedron elements, or a mixture of both types produce more accurate results based on two *a posterior* and one *a priori* metrics.

In addition, two more features of TRUEGRID make it a suitable choice for this AI application. The first is the use of a TRUEGRID command, "write," that allows a user to output executable codes that will run on many FEM platforms such as ABAQUS, ANSYS, LS-DYNA, MPACT, NASTRAN, etc. for the same problem, thus facilitating FEM verification. The second is that the structure of the TRUEGRID language is based on topology, making it ideal to handle a real crack with any irregular shape. The latter is demonstrated in Figs. 6, 7, and 8, where the component with a crack of zig-zag shape is meshed in three stages with a denser mesh always at the new crack tip. The importance of a balanced mesh is also illustrated in Fig. 9.

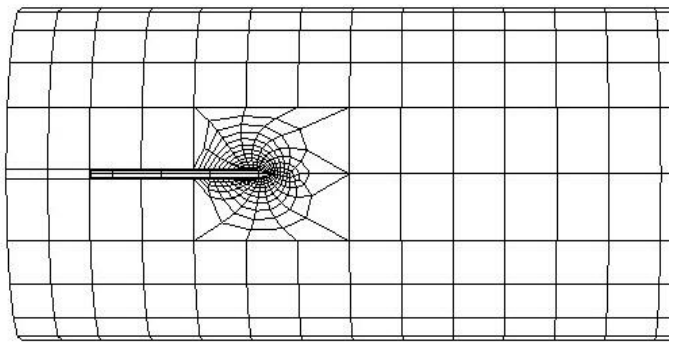

FIGURE 6: Finite element mesh in the neighborhood of a small crack with (a) an all-hexagonal-element-and-optimally-dense-at-crack-tip design, and (b) an automatic re-meshing capability such that when the initial crack length, a_i , is increased to, say, $a_i + d_1$, with d_1 not necessarily collinear with the initial crack, the crack-tip mesh design follows the new crack with the increment, d1 , as shown in Fig. 7.

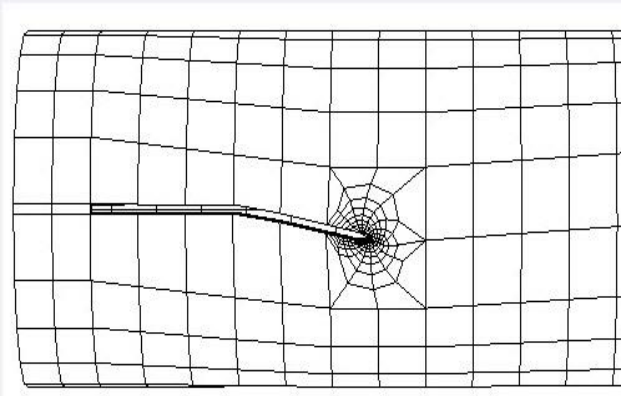

FIGURE 7: Finite element mesh in the neighborhood of a small crack of initial length, a_i , and a first increment of d_1 not collinear with the initial crack but with the crack-tip mesh design same as the initial crack length. Such re-meshing capability is automatic and independent of the angle of orientation of the increment.

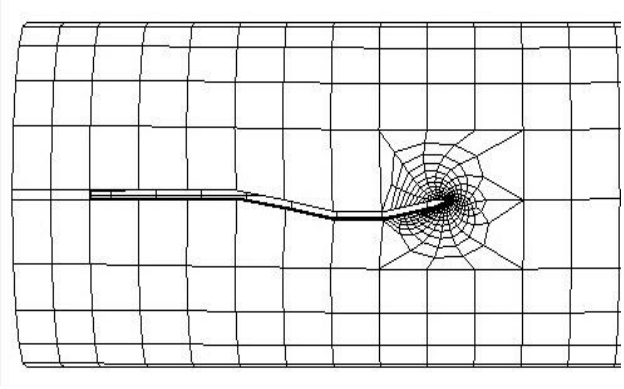

FIGURE 8: Finite element mesh in the neighborhood of a small crack of initial length, a_i , and two increments of d_1 and d_2 not collinear with any of its preceding increment but with the crack-tip mesh design same as the initial crack. Such re-meshing capability is automatic and independent of the angle of orientation of any new increment. Such crack of an irregular shape is called a topological crack, and the algorithm that generates the optimally-dense-crack-tip mesh is furnished by a finite-element-pre-processor named TRUEGRID and its commands based on geometric and topological concepts.

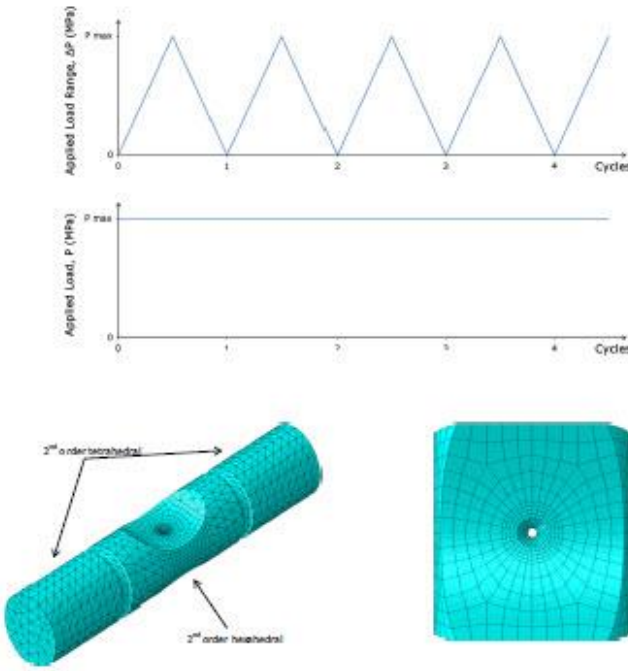

FIGURE 9: A typical representation of a finite element fatigue and static loading history-driven analysis showing the importance of meshing design, where denser mesh is chosen near holes, crack tips, and discontinuities to achieve higher accuracy in stress and strain results (after Beesley, Chen and Hughes [21]).

5. Design of an Intelligent PYTHON (IP) Code

As shown by Chlotte [16], PYTHON is highly suited as a language for writing AI codes in general, because PYTHON code acts as a manager to call on all types of application codes to run on different platforms either sequentially, iteratively, or both.

For example, the following chunk of codes, written in PYTHON, is part of a larger code that will allow a user to run a TRUEGRID application code named "zigzag.tg":

```
Def InverseProgram() :
   self_m_fileInput=True
   print '***  Run TGManager.py '
   total_volume=0.0
   if self_m_fileInput :
      returncode=None
      try :
         z=y[0]+'.tg'
         tg_data=os.path.join(dir_name,z)
         #returncode= call(['C:/TrueGrid/tgd.exe' , zigzag])
         returncode= subprocess.Popen(['C:/TrueGrid/tgd.exe' , zigzag])
         #subprocess.Popen.terminate()
         pass
         if returncode :
            print 'Failure with return code' ,returncode
      except :
         pass
InverseProgram()
```

For the purpose of writing an IP code to turn an SHM data code into a "precision" structural integrity assessment tool by accurately predicting the remaining life of an ageing component, we need to embed in a computing environment the following software packages:

Name of Software	Purpose
(1) PYTHON	(1.1) AI Manager.
(2) DATAPLOT (DP)	3 application codes (2.1) SHM interface. (2.2) Validate m . (2.3) TRUEGRID interface to validate a_f using two FEM platforms.
(3) TRUEGRID	(3.1) Design mesh and output FEM apps.
(4) & (5) Any two of the following FEM codes: ABAQUS, ANSYS, LS-DYNA, MPACT.	(4.1) Interface with (2.3). (5.1) Interface with (2.3).

In the next section, we will show a numerical example of how to validate m using an IP code.

6. A Numerical Example of How to Validate m

We begin our numerical example of how to validate m by repeating below the same tutorial exercise we used in Section 1 with the exception that the initial crack length, a_i , be changed from 1.0 mm to 2.0 mm:

Given: (100 - 106 Material Properties)

(100) AISI 4340 Steel at room temperature.
(104) m = 3.24 (This is the target to be validated)
(105) C_1 = 5.11 x 10^{-10} (unit omitted for brevity).
(106) γ = 0.420.

(200 - 206 Cracked Component Geometry)
(200) A center-cracked plate (see Ref. [2, Fig. 8.12(a)].
(201) b = 38 mm. (202) t = 6 mm.
(203) a_i = 2.0 mm. (This is new.)
(205) d_1 = 1.0 mm. (This is the first increase in a_i after 8,000 cycles (= N_{i1})).
(206) d_2 = 1.0 mm. (This is the second increase in a_i after 4,000 cycles (= N_{i2}- N_{i1})).

(300 - 302 Loading)
(301) P_{min} (minimum applied load) = 80 kN.
(302) P_{max} (maximum applied load) = 240 kN.

To find (c): The correct m after first and second increases.
(d): The remaining life, N_{2f} .

Answer (c):

Step C-101: We first calculate N_{i1} using $m = 3.24$,
$a_i = 2.0$ mm , $a_1 = a_i + d_1 = a_f = 3.0$ mm:
From Eq. (1), $N_{i1} = 13{,}700$ cycles,
which differs from the true N_{i1} (= 8,000 cycles).

Step C-102: We go back to Eq. (1) using $N_{i1} = 8{,}000$ to estimate m . The answer is:

$$m = 3.40.$$

Step C-103: We next calculate N_{i2} using the new $m = 3.40$,
$a_i = 2.0$ mm , $a_2 = a_1 + d_2 = a_f = 4.0$ mm:
Again from Eq. (1), $N_{i2} = 12{,}300$ cycles,
which is very close to the correct N_{i2} (= 12,000).
Therefore, "$m = 3.40$" has been validated. Q.E.D.

Ans. (d): Using $m = 3.40$, we estimate $N_{if} = 22{,}200$ cycles.
Remaining life = $N_{2f} = N_{if} - N_{i2} = 10{,}200$ cycles.

7. Discussion

In this paper, we have narrowed our attention to the effect of the uncertainty of the crack growth exponent on fatigue life, largely because of two new results given by Eqs. (9) and (11), where we show more specifically in Eq. (11) that the effect of the uncertainty of the initial crack length is an order of magnitude smaller than that of the crack growth exponent.

In addition, we did not address the effect of the uncertainty of the crack depth, simply because crack depth is not a parameter in Eq. (1), the governing equation of our fatigue life model. In other words, within the confines of this simple fatigue life model, crack depth and aspect ratio are necessarily ignored. That does not mean they are not important, and the solution is to introduce a more complicated fatigue life model to address them.

It is, however, worthwhile to point out that as a result of this narrowly-restricted investigation, based on the convergence of fast computing power, large database memory, rigorous mathematical and statistical analysis methodologies, multi-scale continuum-fracture-fatigue-creep mechanics and materials science, and advanced sensor technologies, it is now feasible to develop an IP code to bridge the knowledge gap between the state of a new component and that of an ageing one after years of service. The result outlined in this paper is, therefore, significant because it finally allows engineers to design, build, and manage with confidence the operation of any complex structure or system of components as long as adequate SHM systems are in place to utilize the IP code to discover local damage physics and validate predictive simulation models.

However, the IP code designed in this paper does have its limitations, among which the principal one being the assumption that the training sets for deep learning are vast enough to assure convergence of the attempts to validate all of the relevant local material property parameters.

8. Concluding Remarks

An intelligent PYTHON code to utilize the crack length and orientation data from a structural health monitoring (SHM) system mounted on a cracked component, has been designed with the capability of learning from the data to (a) discover local damage physics by an iterative procedure to validate all relevant material property parameters, e.g., the crack-growth exponent, and (b) predict with high confidence the remaining service life of an ageing component. This intelligent code paves the way to the development of a "precision" structural integrity assessment methodology, that is timely and of critical importance to the implementation of a new ASME Boiler and Pressure Vessel Section XI Division 2 Reliability and Integrity Management (RIM) code for inspection of nuclear components [22-24].

ACKNOWLEDGEMENTS

We wish to thank Prof. Fu-Kuo Chang of Stanford University, and Prof. Victor Giurgiutiu of the University of South Carolina-Columbia for their discussion and technical assistance over the last two decades on structural health monitoring. We are also indebted to Prof. Alan Needleman of Texas A & M University, and Prof. Haofeng Chen of the University of Strathclyde, U.K., for their discussion and technical assistance in micro-macro fracture-fatigue-creep modeling in the fall of 2018 when the first author attended their plenary lectures in China. Finally we wish to thank Prof. Shan-Tung Tu of the East China University of Science and Technology, Shanghai, China, for his discussion and encouragement on the development of a new "precision" structural integrity assessment technology.

REFERENCES

[1] Tada, H., Paris, P. C., and Irwin, G. R., 1985, The Stress Analysis of Cracks Handbook, 2nd ed. St. Louis, MO 63105: Paris Productions, Inc. (1985).

[2] Dowling, N. E., 1999, Mechanical Behavior of Materials, 2nd ed. Prentice Hall (1999).

[3] Chang, F. -K., Ed., 2003, Structural Health Monitoring 2003: From Diagnosis & Prognosis to Structural Health Management. Lancaster, PA 17602: DEStech Publications, Inc. (2003).

[4] Giurgiutiu, V., 2008, Structural Health Monitoring with Piezoelectric Wafer Active Sensors, 1st ed. Academic Press (2008).

[5] Fong, J. T., Ranson III, W. F., Vachon, E. I., and Marcal, P. V., 2008, "Structural Aging Monitoring via Web-based Nondestructive Evaluation (NDE) Technology," in Proc. 2008 ASME Pressure Vessels & Piping Division Conference, July 27-31, 2008, Chicago, Illinois, USA, Paper No. PVP2008-61607. American Society of Mechanical Engineers (2008).

[6] Fong, J. T., Marcal, P. V., Hedden, O. F., Chao, Y. J., and Lam, P. -S., 2009, "A Web-based Uncertainty Plug-in (WUPI) for Fatigue Life Prediction Based on

NDE Data and Fracture Mechanics Analysis," in Proc. ASME 2009 Pressure Vessels & Piping Division Conference, July 26-30, 2009, Prague, Czech Republic, Paper No. PVP2009-77827. New York, NY: American Society of Mech. Engineers (2009).

[7] von Euw, E. F. J., Hertzberg, R. W., and Roberts, R., 1972, "Delay Effects in Fatigue-Crack Propagation," in Stress Analysis and Growth of Cracks, ASTM STP 513, pp. 230-259. American Society for Testing and Materials (1972).

[8] Kanninen, M. F., and Popelar, C. H., 1985, Advanced Fracture Mechanics. Oxford University Press (1985).

[9] Fong, J. T., Heckert, N. A., Filliben, J. J., and Doctor, S. R., 2018, "Three Approaches to Quantification of NDE Uncertainty and a Detailed Exposition of the Expert Panel Approach Using the Sheffield Elicitation Framework," in Proc. 2018 ASME PVP Division Conference, Prague, Czech Republic, July 15-20, 2018, Paper No. PVP2018-84771. New York, NY: American Society of Mechanical Engineers (2018).

[10] Ku, H. H., 1966, "Notes on the Use of Propagation of Error Formulas," J. Res. Natl. Bur. Stands., Vol. 70C, No. 4, pp. 263-273 (1966).

[11] Fong, J. T., Hedden, O. F., Filliben, J. J., and Heckert, N. A., 2008, "A Web-based Data Analysis Methodology for Estimating Reliability of Weld Flaw Detection, Location, and Sizing," in Proc. 2008 ASME Pressure Vessels & Piping Division Conference, July 27-31, 2008, Chicago, Illinois, USA, Paper No. PVP2008-61612. New York, NY: Amer. Soc. of Mech. Engineers (2008).

[12] Fong, J. T., and Marcal, P. V., 2009, "A Dataplot-Python-Anlap (DPA) Plug-in for High Temperature Mechanical Property Databases to Facilitate Stochastic Modeling of Fire-Structural Interactions," in Proc. ASME 2009 Pressure Vessels & Piping Division Conference, July 26-30, 2009, Prague, Czech Republic, Paper No. PVP2009-77867. New York, NY: American Society of Mechanical Engineers (2009).

[13] Marcal, P. V., Fong, J. T., and Yamagata, N., 2009, "Artificial Intelligence (AI) Tools for Data Acquisition and Probability Risk Analysis of Nuclear Piping Failure Databases," in Proc. ASME 2009 Pressure Vessels & Piping Division Conference, July 26-30, 2009, Prague, Czech Republic, Paper No. PVP2009-77871. Amer. Society of Mech. Engineers (2009).

[14] Neapolitan, R. E., and Jiang, X., 2018, Artificial Intelligence: With an Introduction to Machine Learning , 2nd ed. Chapman and Hall/CRC (2018).

[15] Boobier, T., 2018, Advanced Analytics and AI: Impact, Implementation, & the Future of Work. Wiley (2018).

[16] Chollet, F., 2017, Deep Learning with Python. Manning Publications (2017).

[17] Frolov, D., 2018, "How Machine Learning Empowers Models for Digital Twins," in BENCHMARK, the International Magazine for Engineering Designers and Analysts from NAFEMS, July 2018 Issue, pp. 48-53 (2018).

[18] Osovski, S., Srivastava, A., Ponson, L., Bouchaud, E., Tvergaard, V., Ravi-Chandar, K., and Needleman, A., 2015, "The effect of loading rate on ductile fracture toughness and fracture surface roughness," J. Mech. Phys. Solids, Vol. 76, pp. 20-46 (2015).

[19] Rainsberger, R., Fong, J. T., and Marcal, P. V., 2016, "A Super-Parametric Approach to Estimating Accuracy and Uncertainty of the Finite Element Method," in Proc. ASME 2016 Pressure Vessels & Piping Division Conference, July 17-21, 2016, Vancoucver, British Columbia, Canada, Paper No. PVP2016-63890. Amer. Soc. of Mech. Engineers (2016).

[20] Rainsberger, R., Fong, J. T., and Marcal, P. V., 2018, "Application of an a priori Jacobian-based Error Estimation Metric to the Accuracy Assessment of 3D Finite Element Simulations," in Proc. ASME 2018 Pressure Vessels & Piping Division Conference, July 15-20, 2018, Prague, Czech Republic, Paper No. PVP2018-84784. New York, NY: American Society of Mechanical Engineers (2018).

[21] Beesley, R., Chen, H., and Hughes, M., 2016, "A novel simulation for the design of a low cycle fatigue experimental testing programme," Computers and Structures, Vol. 178, pp. 105-118 (2016).

[22] ASME, 2018, ASME Boiler and Pressure Vessel Code, Section XI, Division 2 - Requirements for Reliability and Integrity Management (RIM) Program for Nuclear Power Plants, Nov. 11, 2018 Draft for Public Comment. New York, NY: American Society of Mechanical Engineers (2018).

[23] J. T. Fong, J. J. Filliben, N. A. Heckert, D. D. Leber, P. A. Berkman, and R. E. Chapman, 2018,"Uncertainty Quantification of Failure Probability and a Dynamic Risk Analysis of Decision Making for Maintenance of Ageing Infrastructure," to appear in Risk Based Approaches to Complex Systems, P. V. Varde, R. V. Prakash, and N. S. Joshi, Editors, Springer (2018).

[24] Fong, J. T., Heckert, N. A., Filliben, J. J., and Freiman, S. W., 2019, "A Multi-Scale Failure-Probability-based Fatigue or Creep Rupture Life Model for Metal Alloys," to appear in International Journal of Pressure Vessel Technology (2019).